Interaction Thresholds for Adsorption of Quantum Gases on Surfaces and within Pores of Various Shapes†

Hye-Young Kim*

Department of Chemistry and Physics, Southeastern Louisiana University, Hammond, Louisiana 70402

Silvina M. Gatica

Department of Physics and Astronomy, Howard University, 2355 Sixth Street, NW, Washington, DC 20059

Milton W. Cole

Department of Physics, Pennsylvania State University, University Park, Pennsylvania 16802

Received: June 5, 2007; In Final Form: August 10, 2007

Adsorption within pores and on surfaces occurs because of the attractive potential provided by the adsorbent. If the attraction is too weak, however, adsorption does not occur to any significant extent. This paper evaluates the criterion for such adsorption, at zero temperature, of the quantum gases ^{4}He and H_2. This criterion is expressed as a relationship between a threshold value of the well-depth (D) of the adsorption potential (on a semi-infinite planar surface) and the hard-core diameter (σ) of the gas-surface pair potential. Six geometries are considered, of which two result in two-dimensional (2D) adsorbed phases, two result in one-dimensional (1D) phases, and two result in zero-dimensional phases. These are monolayer films on semi-infinite substrates or within a slit pore, linear or axial phases within cylindrical pores (within bulk solids) or cylindrical tubes, and single-particle adsorption within spherical pores or hollow spherical cavities, respectively. The criteria for film adsorption are consistent with analogous criteria for film wetting to occur, evaluated with a simple thermodynamic model.

1. Introduction

The subject of adsorption has been studied for more than a century, resulting in a vast body of experimental and theoretical information about the behavior of various gases on surfaces and within pores, varying in composition and morphology.[1−3] Many macroscopic and even mesoscopic aspects of this behavior can be understood from general thermodynamic principles, like Kelvin's equation. At the nanoscale, however, a quantitative theoretical understanding of a specific system requires explicit evaluation of the appropriate equations of statistical mechanics, incorporating the relevant interactions. These are the gas−gas and gas−surface interactions. Knowing these interactions, in principle, one can predict the adsorption behavior, including the structural, thermodynamic, and dynamical properties of films.

Since the variety of possible adsorption systems is great, general principles or guidelines are useful for anticipating what adsorption behavior will occur in a particular circumstance, for example, the pressure at which a monolayer film occurs at a specified temperature. There exists a number of generic models (e.g., Langmuir and BET) that achieve this goal semiquantitatively. This paper addresses an analogous, but more restricted, problem. This is the determination of whether or not a given geometry and substrate material provides a sufficiently attractive adsorption potential for a film to appear, below saturated chemical potential, at zero temperature. By focusing on temperature $T = 0$, and hence the ground state of the system, a significant simplification occurs in the analysis of this problem. We focus further on two specific adsorbates, ^{4}He and H_2, each of which requires a quantum treatment. This choice is motivated, in part, by the fact that a large body of prior experimental and theoretical study has addressed the low-T adsorption of these gases in planar or cylindrical geometries.[4−8] Particular attention has focused on the ^{4}He case because of the superfluid behavior, present even in monolayer films. Once believed[9] to be a "universal wetting agent" because of its weak cohesion, ^{4}He films became even more interesting with the discovery of wetting transitions on weak-binding substrates.[3,5,7,10−16] The criteria for the occurrence of these transitions are closely related to those found in the present calculations. This is not a coincidence; both involve a competition between cohesive and adhesive interactions. For systems exhibiting wetting transitions, the adsorption potential is too weakly attractive to yield significant adsorption at low T (the wetting transition occurs at high T, entropy-driven). Such systems include the inert gases and H_2 adsorbed on alkali metal surfaces. Relatively accurate values of the interaction parameters are known in these cases, which are therefore convenient to have for the present study.[16,17] These weak-binding systems, not surprisingly, are found to have interactions that straddle the crossover criteria derived in the present paper for the various geometries of interest. Thus, cases of very weak attraction between the gas and the surface are likely to result in both nonwetting behavior and the absence of monolayer adsorption.

This dependence of the adsorption behavior on the gas−surface interaction has been investigated previously in many

† Part of the "Giacinto Scoles Festschrift".

* To whom correspondence should be addressed. E-mail: Hye-Young.Kim@selu.edu.

10.1021/jp074354p CCC: $37.00
Published on Web 09/26/2007

ways. Among these are simulation studies concerned with classical fluids in slit and cylindrical pores at finite temperature. Closely related to the present paper is a recent study of classical adsorption at $T = 0$ in a variety of geometries.[18] A general characteristic of these approaches is the incorporation of the explicit gas−surface interaction to complement the thermodynamic description.

The following section addresses quasi-two-dimensional (2D) adsorption of monolayer films in two environments. One is a semi-infinite substrate with a flat surface, a geometry which has attracted the majority of theoretical studies in the past. The other is a slit-shaped pore, bound by two half-spaces with parallel faces. We refer to this as the "sandwich geometry". For each geometry and each of the two adsorbates, we determine the criterion for the film to exist at a value of the ground-state's chemical potential $\mu < \mu_0$, where μ_0 corresponds to that of the bulk adsorbate at $T = 0$. This criterion is expressed in terms of the adsorption potential, $V(z)$, which we evaluate by integrating $U_{gs}(r)$, Lennard-Jones two-body interactions between the adsorbate and the substrate atoms. Specifically, the criterion expresses a relationship between a threshold value of the well depth of the adsorption potential and the hard-core distance (σ) in the interatomic potential $U_{gs}(r)$. If the well depth for the actual system of interest exceeds this threshold value, then monolayer adsorption will occur at $T = 0$, beginning at some $\mu < \mu_0$; otherwise, no such adsorption occurs. In the slit-pore geometry, the threshold well depth turns out to be about one-half of the value for a single surface (because the adjacent media are assumed to contribute additively). In finding this threshold value, we maximize the film's binding by an appropriate choice of the separation L between the two surfaces.

Section 3 is concerned with quasi-1D adsorption, associated with a line of adsorbate atoms. The specific geometries explored are a cylindrical tube (e.g., single-wall carbon nanotube), made of one atomic layer of matter, and a cylindrical pore within an otherwise solid material. In each case, we treat the cylinder radius R as a free parameter. For a given value of σ, we find the "optimized" R, such that the adsorbed film's energy is a minimum. We then evaluate the well-depth criterion for such a 1D film to exist. Section 4 discusses a (more academic) spherical geometry. Results are obtained for a spherical pore and a hollow spherical cavity. The threshold values of the well depth are presented in terms of the well depth (D) of the atomic adsorption potential on a semi-infinite planar surface in all cases except the cylindrical tube and the spherical shell, for which the threshold value is presented in terms of the well depth (D_{sheet}) of the atomic adsorption potential on a monolayer flat substrate. Section 5 summarizes our results.

2. Quasi-2D Phases

2.a. Monolayer Film Adsorbed on a Half-Space. In this section, we evaluate the criterion for the existence of a planar, monolayer film at a chemical potential (μ) below the saturation value μ_0. The first substrate geometry to be considered is a half-space, $z < 0$, occupied by a continuum, uniform material with atomic number density n. For an adatom located at distance z above this surface, the potential is obtained by integrating over the substrate the venerable Lennard-Jones (LJ) 6-12 interaction, $U_{gs}(r)$, with hard-core diameter and well-depth interaction parameters σ and ϵ, respectively. The result of such integration is a 3-9 adsorption potential

$$V(z) = \frac{2\pi n\epsilon\sigma^3}{3}\left[\frac{2}{15}\left(\frac{\sigma}{z}\right)^9 - \left(\frac{\sigma}{z}\right)^3\right] \tag{1}$$

Then, the position z_{min} of the minimum, the well depth $D = -V(z_{min})$, and the force constant $k = V''(z_{min})$ are the following

$$z_{min} = \left(\frac{2}{5}\right)^{1/6}\sigma \tag{2}$$

$$D = \frac{2\sqrt{10}\,\pi n\epsilon\sigma^3}{9} \tag{3}$$

$$k = \left(\frac{5}{2}\right)^{5/6}(12\pi n\epsilon\sigma) = \frac{\alpha D}{\sigma^2} \tag{4}$$

Here, $\alpha = k\sigma^2/D = 27(5/2)^{1/3} \approx 36.64$. We now address the question of whether or not a monolayer film forms on this surface (at $T = 0$, $\mu < \mu_0$). The criterion is that the ground-state energy per particle of the film (E_{film}) is smaller than that of the bulk material (E_{3D}). For the former quantity, we decompose it into a surface-normal part, the energy per particle of a single adsorbed molecule (E_1), plus a tangential part, the many-body energy per particle (E_{2D}) of a free-standing, 2D film, in the absence of a holding potential

$$E_{film} = E_1 + E_{2D} \tag{5}$$

$$E_{film} = -D + \frac{\hbar\omega}{2} + E_{2D} \tag{6}$$

In the preceding equation, we adopt the harmonic approximation so that the zero-point energy is $\hbar\omega/2$, where $\omega = \sqrt{k/m}$. We have confirmed the accuracy of this approximation (within 1% for the present case) by comparing with exact results for the present circumstance, obtained previously for the 3-9 potential.[19] Combining the preceding equations, we determine the threshold criterion by setting $E_{film} = E_{3D}$, the upper limit for the existence of the film. This equality may be written as

$$E_{3D} - E_{2D} = -D + \left(\frac{\hbar}{2\sigma}\right)\sqrt{\frac{\alpha D}{m}} \tag{7}$$

For the specific adsorbates, ^{4}He and H_2, we know the left side of this equation from existing experiments (E_{3D}) and/or calculations (E_{2D}). With these data as input, we use eq 7 to evaluate the threshold value of D as a function of the variable σ. The specific values employed are the following for ^{4}He (H_2): $E_{3D} = -7.17(-89.8)$K and $E_{2D} = -0.85(-23.4)$K.[20−23] The results derived from eq 7 are shown in Figures 1 and 2, for ^{4}He and H_2, respectively. The range of σ values in these figures is typical of gas−surface interactions. The points shown on these graphs pertain to various weakly attractive adsorption systems, those studied in the context of wetting transitions; we return to this relationship in the next subsection. Note, for comparison, that graphite, the most attractive surface exhibiting physical adsorption, would be represented by a point far above the threshold curve, with an estimated D close to 200K for ^{4}He and 600K for H_2[24−26].

We address one point about the approximation of energy additivity, expressed in eq 5. The addition of a surface-normal (z) energy of a single particle and the surface-parallel (xy) many-body energy neglects the fact that these degrees of freedom are weakly coupled; that is, the z motion affects the mutual interaction energy present in the xy problem. This approximation was assessed for He adsorption on flat surfaces by Annett et al.,[26] who found energy shifts on the order of 1K, or less, to result from the coupling of these motions. We omit that correction from the present analysis.

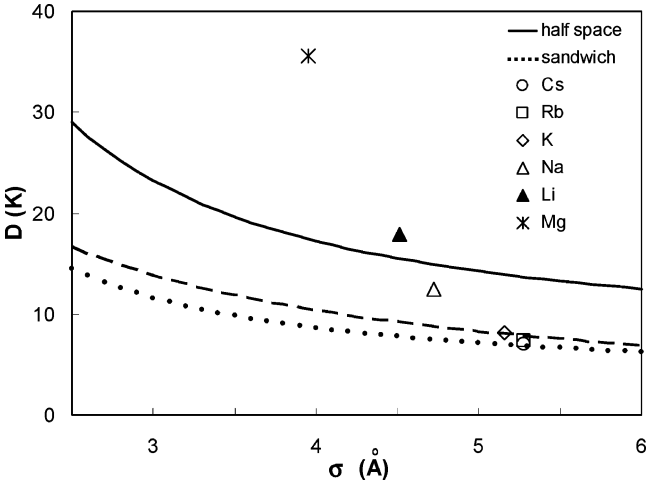

Figure 1. Threshold value of D for ^{4}He monolayer formation in the half-space (full curve) and sandwich (dots) geometries as a function of the gas−surface interaction's hard-core diameter σ. The dashed curve corresponds to the simple model's prediction of the ^{4}He wetting transition for a single surface, eq 10. Points for various surfaces are taken from ref 16. D is the well depth of the atomic adsorption potential on a flat, half-space substrate.

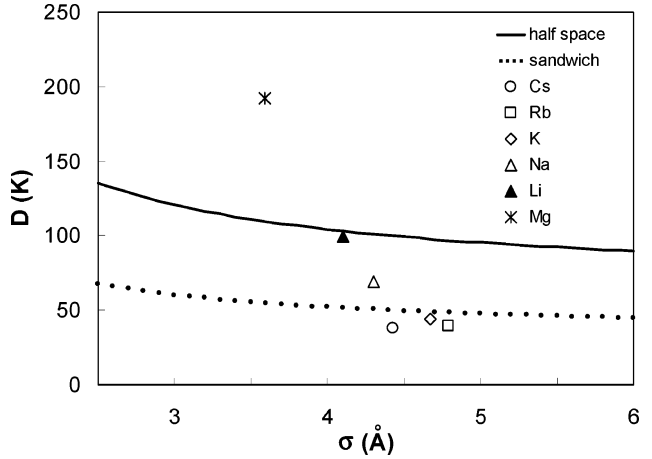

Figure 2. Threshold values of D for H_2 monolayer formation in the half-space (full curve) and sandwich (dots) geometries as a function of the gas−surface interaction's hard-core diameter σ. Points for various surfaces are taken from refs 16 and 17.

According to the present model, among the systems shown in Figure 1, only Li and Mg should adsorb monolayer films of ^{4}He at $T = 0$. In contrast, K, Na, Rb, and Cs should not adsorb such a film, meaning that these surfaces are bare of ^{4}He at saturation, for $T = 0$. While this finding is consistent with experimental data for Cs, the existing data for Rb are ambiguous, as discussed below.[27−29]

We could, in principle, present a figure analogous to Figure 1 for the case of ^{3}He adsorption. ^{3}He, too, has a wetting transition on Cs.[30] Since the potentials are the same for both isotopes, there would arise just two differences from the ^{4}He case. One is that the zero-point energy would be larger by a factor of $\sqrt{4/3} \approx 1.15$. The second is that the ^{3}He film is unbound in 2D.[31] The former difference would increase the middle term in eq 6 by about 1K, and the latter would increase the right-most term by 0.85K. Together, these differences would result in an upward shift in the ^{3}He threshold for the half-space substrate by nearly 2K relative to that of ^{4}He. Thus, the existence of a ^{3}He monolayer on Li is a marginal case, while the ^{4}He monolayer film is definitely predicted to exist on Li. The latter result was previously found to be the case with both exact (diffusion Monte Carlo) and approximate (density functional model) calculations.[32]

For H_2, shown in Figure 2, as compared to He, there are fewer adsorption studies or detailed calculations to test the present model.[11,33−35] Note that those surfaces (alkali and alkaline earth metals) which are weakly attractive for ^{4}He adsorption are also weakly attractive for H_2. At the extreme limit of ultraweak interaction, the surfaces of Rb and Cs have both shown very small adsorption of ^{4}He at low T. H_2 exhibits negligible adsorption on Rb and Cs at 15 K, followed by wetting transitions on both surfaces near 20 K. This behavior corresponds, within 20%, to the simple model's predictions based on well depths D near 40−50 K.[16,35]

2.b. Relation to the Wetting Transitions. As mentioned earlier, the wetting transition is closely related to the problem investigated in this paper, the existence of the monolayer film at saturation. We quantify the relationship here. At $T = 0$, the criterion distinguishing between (complete) wetting and nonwetting (partial wetting) behaviors differs from the monolayer criterion by the substitution of the bulk liquid for the monolayer film. In principle, a situation can occur in which a monolayer exists without complete wetting;[36] alternatively, complete wetting can occur without there existing a monolayer phase. A phenomenological criterion for ^{4}He wetting was proposed by Cheng et al.; subsequently, this criterion was found to be accurate for this and other simple fluids.[7,15,32,34,36] Called the "simple model", the criterion relates threshold values of the adsorption interaction parameters (D and C_3, the well depth and the coefficient of the asymptotic z^{-3} adsorption potential, respectively) to thermodynamic properties of ^{4}He, σ_{lv} and n_{liq}, the interfacial tension and liquid density, respectively, at $T = 0$. Wetting occurs in this model if

$$(C_3D^2)^{1/3} > 3.33\,\frac{\sigma_{lv}}{n_{liq}} = 3.33\,\frac{0.268\text{K/Å}^2}{0.0218/\text{Å}^3} = 40.9\text{K·Å} \qquad (8)$$

Writing

$$\frac{C_3}{D} = \frac{(2\pi n\epsilon\sigma^6/3)}{\sqrt{5/2}\,(4\pi n\epsilon\sigma^3/9)} = \frac{3}{\sqrt{10}}\,\sigma^3 \qquad (9)$$

The wetting criterion for ^{4}He becomes

$$D\sigma = 41.6\text{K·Å} \qquad (10)$$

The corresponding curve is observed in Figure 1 to fall close to the threshold criterion for the sandwich geometry but significantly below the single surface monolayer curve. This means that systems with interaction parameters lying between this wetting curve and the monolayer curve do not exhibit a monolayer film on a single surface, according to this model. Yet, such systems do exhibit wetting behavior at $T = 0$; they do so by having a discontinuous isotherm (coverage as a function of chemical potential) at low T, with two or more layers forming simultaneously as μ reaches a transition value (somewhere below μ_0). An experimental realization of this behavior is ^{3}He/Cs, which exhibits such a discontinuity at low T.[37] The systems ^{4}He on Rb and Cs are seen in Figure 1 to fall just below the wetting curve. This finding is consistent with ^{4}He/Cs exhibiting nonwetting behavior at low T and a wetting transition at nonzero T. For ^{4}He/Rb, the experimental evidence concerning the $T = 0$ wetting behavior is contradictory, with different groups reaching different conclusions.[27−29]

Concerning the problem of ^{3}He wetting, to analyze that problem, the right-hand side of eq 10 would be replaced by the value 23K·Å, different because the $T = 0$ surface tension and density are very different from those of ^{4}He. A curve representing the wetting criterion for ^{3}He would show the threshold value of D to be about one-half of that for ^{4}He. From such a model, one would conclude that all known surfaces are wet by ^{3}He at $T = 0$. This finding is consistent with detailed calculations and experiments.[30] Note that the threshold for monolayer formation on ^{3}He is higher than that for ^{4}He, while the reverse relationship is found for the wetting thresholds.

2.c. Sandwich Geometry. Turning to the sandwich geometry, we explore the criterion for a monolayer film to adsorb within a slit pore, defined by two half-spaces, denoted A and B, with parallel faces. These are separated by a distance L, which we vary in order to minimize the energy. As in the preceding discussion, we search for the most strongly bound phase of a monolayer film. Ignoring many-body effects, as is conventional, the total potential energy experienced by the adparticle is taken to be the sum of contributions from the two adjacent materials.[38]

Then, for an atom at distance z from one surface, A, the total potential energy is

$$V_{\text{slit}}(z) = V_{\text{A}}(z) + V_{\text{B}}(L - z) \tag{11}$$

In the case of identical media binding the slit, the potential energy assumes one of two qualitatively distinct forms, depending on the ratio $L^* = L/\sigma$. If $L/2$ exceeds the distance to the inflection point ($z_{\text{inflection}} = \sigma$) of $V_{\text{A}}(z)$, the single surface potential, then the total potential energy $V_{\text{slit}}(z)$ has two equivalent minima, one near each surface. In such a case, the double-well geometry yields the well-known splitting of otherwise degenerate states. Otherwise, $V_{\text{slit}}(z)$ has a single minimum located at the midpoint of the slit. Thus, the criterion for a single minimum is $L^* < 2$. Our focus is the strongest binding, which occurs in the latter case.

To determine the most strongly bound film, one recognizes that this occurs when z is taken to be the equilibrium position for surface A (i.e., $z = (z_{\text{min}})_{\text{A}}$) and sets $L - z = (z_{\text{min}})_{\text{B}}$, the equilibrium distance for substrate B. In this optimized case, then, $L = (z_{\text{min}})_{\text{A}} + (z_{\text{min}})_{\text{B}}$. The force constant for this potential (k_{slit}) is seen to be the sum of the force constants for the two surfaces, k_{A} and k_{B}, $k_{\text{slit}} = k_{\text{A}} + k_{\text{B}}$. For simplicity, we consider subsequently the case of two identical media, so that $L = 2(z_{\text{min}})_{\text{A}}$. Then, the resulting well depth is twice that of the single surface (i.e., 2D), as is the force constant. The analysis of this situation proceeds like that of the single surface case, with the resulting criterion given by an appropriately modified version of eq 7

$$E_{\text{3D}} - E_{\text{2D}} = -2D + \frac{\hbar}{\sigma}\sqrt{\frac{\alpha D}{2m}} \tag{12}$$

If we were to ignore the zero-point term, the threshold value of D for this sandwich geometry would be one-half of that of the single surface. Because of this term, instead, the threshold value is somewhat more than half, as seen in Figures 1 and 2. Note that the cases of Cs, Rb, and K are ones for which no monolayer film exists in the sandwich geometry for H_2, while for ^{4}He, there are just the marginal cases of Rb and Cs that just might exclude this monolayer film, but the uncertainty of the parameter values is too large to be sure.

In the preceding discussion, we have fixed the value of L by minimizing the potential energy alone. A more complete analysis is discussed in the Appendix, where the energy minimization yields an approximately 20% larger value of L than that of the relation $L = 2z_{\text{min}}$ based on the potential energy alone. Qualitatively, the wider pore reduces the zero-point energy somewhat, without sacrificing the potential energy significantly.

3. Quasi-1D Phases Confined within Cylindrical Surfaces

3.a. Criterion for 1D Phases. Because of numerous studies of adsorption inside and outside of various kinds of nanotubes, there is particular interest in the threshold criteria for this geometry. In this section, we consider first endohedral adsorption within the single-wall tube, and then address the problem of a cylindrical pore within a solid material. We focus on the problem of the adsorption of a linear, or axial, phase within this environment. Apart from the 1D character of the problem, the concepts are qualitatively similar to those of the previous section. The goal remains one of identifying the optimal geometry (here, the radius R of the cylinder) for maximum binding of the film. The threshold condition is thus given in terms of the 1D energy per particle, E_{1D}, by

$$E_{\text{3D}} = E_{\text{1D}} + \min\{V_{\text{min}} + \hbar\omega_{\text{r}}\} \tag{13}$$

In this case, the potential energy is expanded about the axial value, $V(r = 0; R)$, with a radial force constant k_{r}, as

$$V(r) = V(r = 0; R) + \frac{1}{2}k_{\text{r}}r^2 \tag{14}$$

There being two transverse (radial) degrees of freedom in the pore, the quantity $\hbar\omega_{\text{r}}$ is the zero-point energy, where $\omega_{\text{r}} = \sqrt{k_{\text{r}}/m}$. Analysis based on eq 13 requires input values of E_{1D} at $T = 0$. These have been calculated to be about $E_{\text{1D}} = -1.7$mK for ^{4}He and $E_{\text{1D}} = -4.834$K for H_2.[39,40]

3.b. Cylindrical Tube. The calculations of the potential energy within a cylindrical tube have been carried out by Stan and Cole, with these results for $V(r = 0; R)$, the potential energy on axis, and the radial force constant k_{t}:[41]

$$V(r = 0; R) = 3\pi^2\theta\epsilon\sigma^2\left[\left(\frac{21}{32}\right)\left(\frac{\sigma}{R}\right)^{10} - \left(\frac{\sigma}{R}\right)^4\right] \tag{15}$$

$$k_{\text{t}} = 3\pi^2\theta\epsilon\left[\left(\frac{2541}{32}\right)\left(\frac{\sigma}{R}\right)^{12} - 25\left(\frac{\sigma}{R}\right)^6\right] \tag{16}$$

Here, θ is the 2D density of atoms comprising the tube, assumed to be constant, that is, a continuum substrate. This expression for the axial potential has a minimum when $R_{\text{min}} = (105/64)^{1/6}\sigma \approx 1.086\sigma$, at which point the potential and force constant become

$$V_{\text{min}} = V(r = 0; R_{\text{min}}) = -\frac{144\pi^2}{5(105)^{2/3}}\theta\epsilon\sigma^2 \tag{17}$$

$$k_{\text{t}} \approx 422.3\theta\epsilon \tag{18}$$

These expressions can be related to the well depth for the case of adsorption on a hypothetical monolayer substrate (like graphene). In that case, the potential energy obtained by integration over the (assumed continuum) sheet has a well-depth value (at $z_{\text{min}} = \sigma$) of

$$D_{\text{sheet}} = \frac{6\pi}{5}\theta\epsilon\sigma^2 \tag{19}$$

From eqs 13, 17, and 18, we see how the V_{min} and ω_{r} parameters present in eq 13 can be expressed in terms of the alternative

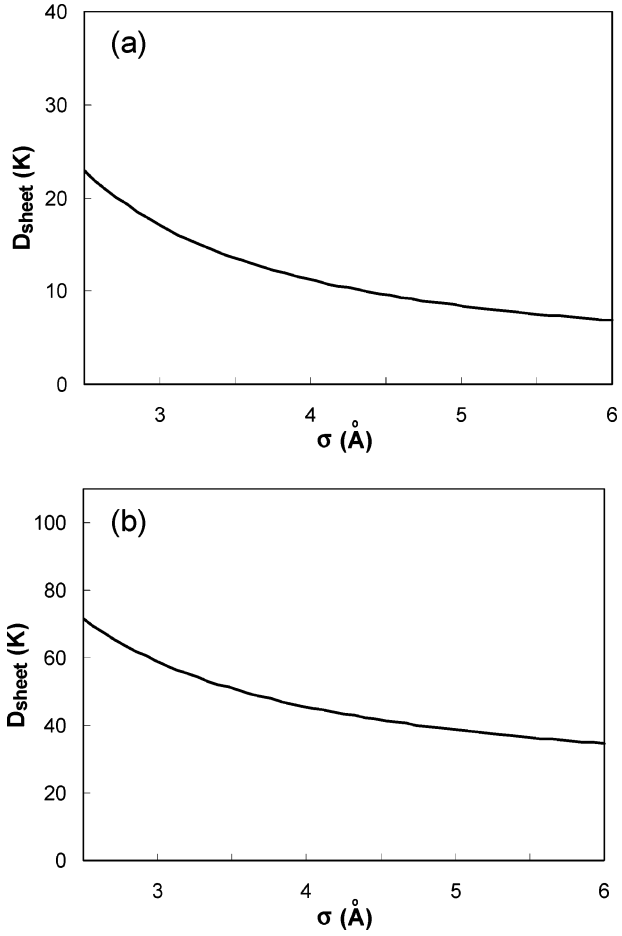

Figure 3. Threshold criterion (D_{sheet} as a function of σ) for the existence of 1D phases of ^{4}He (a) and H_2 (b) within a cylindrical tube at $T = 0$. D_{sheet} is the well depth of the atomic adsorption potential on a flat, monolayer substrate.

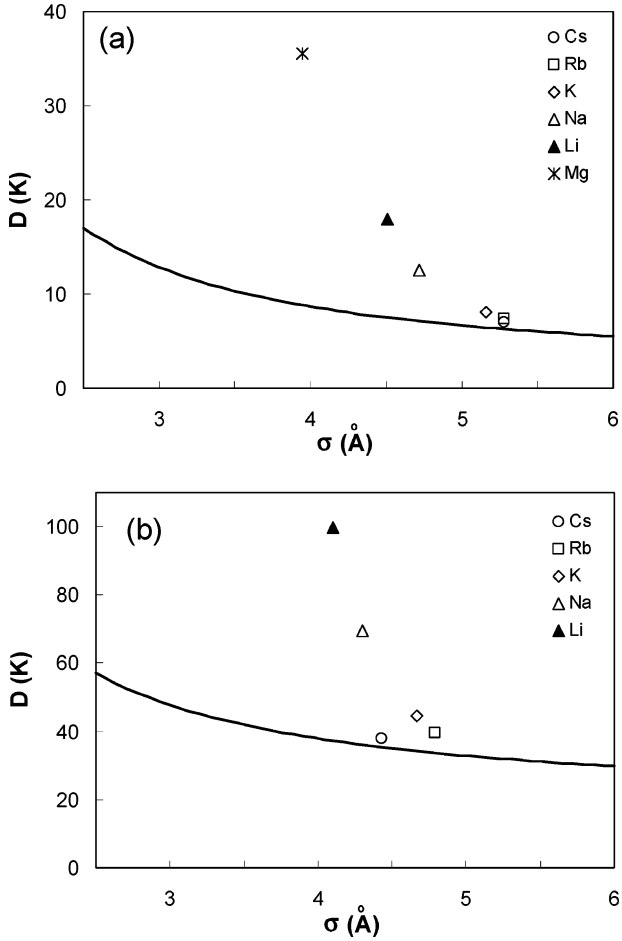

Figure 4. Threshold value of D for existence of an axial phase inside of a cylindrical pore for ^{4}He (a) and H_2 (b) as a function of σ, the gas−surface interaction's hard-core diameter. Points are interaction parameters of refs 16 and 17.

parameters D_{sheet} and σ. The resulting axial phase criterion, eq 13, can be expressed as a relation between D_{sheet} and σ. This approach yields the numerical results shown in Figure 3 for ^{4}He and H_2.

3.c. Cylindrical Pore. The procedure in the case of a cylindrical pore is analogous to that discussed in section 2, apart from geometrical details. We have derived the following results by integrating the LJ pair interaction over the solid. Let r denote the distance from the axis so that $V_R(0)$ is the potential on the axis. For small r, an expansion yields

$$V(r) = V_R(0) + \frac{1}{2} k_p r^2 \tag{20}$$

$$V_R(0) = \pi^2 n\epsilon\sigma^3 \left[\frac{7}{32}\frac{1}{x^9} - \frac{1}{x^3}\right] \tag{21}$$

$$k_p = \pi^2 n\epsilon\sigma \left[\frac{10.83}{x^{11}} - \frac{1.875}{x^5}\right] \tag{22}$$

Here $x = R/\sigma$ is the reduced radius. The axial potential energy has a minimum value (V_{min}) at $x_{min} = R_{min}/\sigma = (21/32)^{1/6} \approx 0.932$, given by

$$V_{min} = -8.122 n\epsilon\sigma^3 \tag{23}$$

This value can be compared with the well depth above a semi-infinite half-space, with a planar surface $D = (2\pi\sqrt{10}/9)n\epsilon\sigma^3$. Numerically, the ratio $|V_{min}|/D = 3.68$, showing the greater coordination inside of a cylindrical pore compared to that of a flat surface. The force constant for this optimal radius R_{min} has a value of

$$k_p = 205.4 n\epsilon\sigma = \frac{(205.4)(9)}{2\pi\sqrt{10}} \frac{D}{\sigma^2} \approx 92.9 \frac{D}{\sigma^2} \tag{24}$$

Using the ratio 3.68 from above, the relevant criterion for forming the axial phase is this (analogous to eq 13)

$$E_{3D} - E_{1D} = -3.68D + \frac{\hbar}{\sigma}\sqrt{\frac{92.9D}{m}} \tag{25}$$

Figure 4 compares numerical values of this criterion inside of pores for ^{4}He and H_2. The key finding is that the energetic benefit of the high coordination within a cylinder is to reduce the threshold value of D considerably below the values found for half-space and close to the values for the slit-pore geometry. Specifically, for ^{4}He, the D threshold (at a given value of σ) in the pore geometry is within 10% of the threshold for the sandwich geometry. For H_2, the pore threshold values of D are about 2/3 of those for the sandwich geometry. The similarity of the thresholds in the sandwich and pore geometries occurs because the significantly greater attraction in the pore is approximately compensated for by the smaller cohesive energy in 1D than that in 2D. Note that the theoretical well depth for

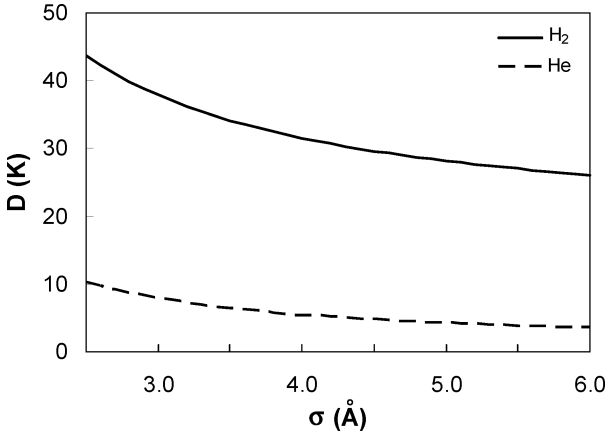

Figure 5. Threshold value of D as a function of the gas−surface interaction length, σ, shown for the case of adsorption within a spherical pore. Results are shown for H_2 (full curve) and ^{4}He (dashes).

^{4}He/Cs is sufficient to yield the 1D axial phase within a pore, although it is not sufficient to adsorb a monolayer film on a flat surface, according to Figure 1.

4. Spherical Geometry

We now turn to the spherical geometry, which leads to a zero-dimensional situation, that is, matter localized at, or near, the center of the sphere (at the origin). Although cylindrical models have been used often to treat porous media, the actual geometry is sometimes closer to spherical. As a result, spherical cavities have indeed been explored previously as a host environment for adsorption. Early works on this subject include, for example, refs 38, 42, 43, and 44. Currently studied examples of such porous media include fullerenes and "inverse opal materials".[45] We ignore the computational details and present just the results in two geometries analogous to those of the cylindrical problem, a spherical pore or a hollow sphere. Here, with the LJ interaction, we express results in terms of the van der Waals coefficients, $C_{12} = 4\epsilon\sigma^{12}$ and $C_6 = 4\epsilon\sigma^6$. For a spherical cavity of radius R, the potential energy $V_{\text{sphercav}}(r)$ satisfies

$$V_{\text{sphercav}}(r) = 4\pi n \left\{ \frac{C_{12}}{45R^9} \frac{F(\rho)}{(1-\rho^2)^9} - \frac{C_6}{3R^3(1-\rho^2)^3} \right\} \tag{26}$$

$$F(\rho) = 5 + 45\rho^2 + 63\rho^4 + 15\rho^6 \tag{27}$$

Here, $\rho = r/R$ is the reduced radial distance. At the origin, this expression reaches a value of

$$V_{\text{sphercav}}(r=0) = V(0) = \frac{4\pi n}{9}\left[\frac{C_{12}}{R^9} - \frac{3C_6}{R^3}\right] \tag{28}$$

This function is a minimum at $R_{\text{min}} = (C_{12}/C_6)^{1/6}$, which, for the LJ potential, yields $R_{\text{min}} = \sigma$. Hence, the global minimum potential energy is

$$V_{\text{min}}(0) = -\left(\frac{32\pi}{9}\right) n\epsilon\sigma^3 \tag{29}$$

This value differs from that for a cylindrical pore, for which the numerical factor, 8.122, is smaller than $(32\pi/9) = 11.17$ by a factor 1.4, a consequence of the higher coordination in the spherical case. The threshold criterion for the spherical geometry to exhibit adsorption is simply found from the substrate potential energy field since we may assume there is just a single adsorbed particle for this "point phase" of matter. The criterion for its existence is

$$E_{\text{3D}} = V_{\text{sphercav}}(R_{\text{min}}) + \frac{3\hbar}{2}\sqrt{\frac{k_{\text{sphercav}}}{m}} \tag{30}$$

Here, k_{sphercav} is the force constant in the spherical potential. Its dependence on R is given by the following expression

$$k_{\text{sphercav}}(R) = 8\pi n\left(\frac{2C_{12}}{R^{11}} - \frac{C_6}{R^5}\right) \tag{31}$$

At the optimized value $R_{\text{min}} = \sigma$, this yields $k_{\text{sphercav}}(R) = 32\pi n\epsilon\sigma$. Figure 5 shows the resulting criterion for adsorption in this pore. Not surprisingly, the threshold value of D is smaller than that found for the other geometries. The very high coordination of the spherical environment allows adsorption at its center for all known materials.

For completeness, we address one additional geometry, a hollow spherical shell. In this case, the potential energy is

$$V_{\text{hollow}}(r) = 4\pi\theta\left\{\frac{C_{12}}{5R^{10}}\frac{H(\rho)}{(1-\rho^2)^{10}} - \frac{C_6}{R^4}\frac{(1+\rho^2)}{(1-\rho^2)^4}\right\} \tag{32}$$

$$V_{\text{hollow}}(r) = 4\pi\theta\left(\frac{C_{12}}{5R^{10}}H(\rho) - \frac{C_6}{R^4}\frac{(1+\rho^2)}{(1-\rho^2)^4}\right) \tag{33}$$

$$H(\rho) = 5 + 60\rho^2 + 126\rho^4 + 60\rho^6 + 5\rho^8 \tag{34}$$

In this situation, the potential energy at the origin is a minimum when $R/\sigma = (5/2)^{1/6}$, at which point one finds $-V_{\text{min}} \approx 16.4\theta\epsilon\sigma^2$. The force constant in this optimized case is $k_{\text{hollow}}(r) \approx 153\theta\epsilon$. The numerical factor in the holding potential V_{min} is nearly 30% larger than the value (12.8) obtained (eq 17) for the cylindrical tube geometry. In both this case and the spherical cavity case, the enhanced substrate attraction (relative to the other geometries) implies a lower threshold for the planar surface well depth D than for the previously considered cases.

5. Summary and Conclusions

In this paper, we have investigated a conceptually straightforward question: do there exist quasi-0D, -1D, or -2D phases of the quantum gases ^{4}He and H_2 near a set of specific surfaces? The answers to this question depend on two parameters entering the gas−surface interaction. We can find these answers relatively easily because we let $T = 0$ and because we exploit existing information about the energies of the free-standing 1D or 2D phases of these materials. The total energy includes also the potential energy provided by the host substrate, along with the zero-point energy associated with fluctuations about the equilibrium 1D or 2D structures.

For the quasi-2D half-space geometry, the threshold criterion for the well depth (D) for monolayer formation, at fixed σ, is seen in Figure 1 to exceed, by a factor ~2, the "simple model" criterion for wetting on the same surface. This result is expected because films can wet a surface without forming a monolayer, as occurs for the ^{3}He/Cs case. In contrast, as is also expected, the wetting criterion for D is less stringent than the criterion for a film to exist in the optimized sandwich geometry.

The well-depth criteria for quasi-1D ^{4}He and H_2 films to occur within cylindrical or spherical tubes and pores are comparable to those found for the sandwich geometry. This conclusion is derived by assuming that one has the freedom to design a pore or tube of the optimal radius and comparing the results with

those for a sandwich geometry with optimized spacing L between the half-space substrates. If this optimization is not applicable, then one can evaluate the criterion for a specific R and L, using the same approach as that outlined here, employing the appropriate formulas above for the specific geometry.

Acknowledgment. We are grateful to NSF for support of this research, to Susana Hernández for helpful comments, and to Alberto Hernando de Castro, of the University of Barcelona, for computing H_2−surface interactions at our request.

Appendix: Zero-Point Energy in the Sandwich Geometry

In this section, we evaluate the effect on the slit-pore's width (L) of including the zero-point energy (ϵ) on the energy minimization with respect to L. For the (symmetrical) case where opposite sides of the "sandwich" are made of the same material, the particle's equilibrium position lies halfway between the two walls, at distance z. Then, the energy $E(z)$ is a sum of the potential energy at the equilibrium position and ϵ

$$E(z) = 2V(z) + \epsilon(z) \tag{A1}$$

$$\epsilon(z) = \frac{\hbar}{2}\sqrt{\frac{2k(z)}{m}} \tag{A2}$$

Here, $k(z) = V''(z)$ is the second derivative of the potential energy contributed by a single half-space. Seeking to minimize the total energy, by differentiating, we get a perturbative expansion

$$0 = 2V'(z) + \epsilon'(z) \approx 2[V'(z_{\min}) + (z - z_{\min})V''(z_{\min})] + \epsilon'(z_{\min}) \tag{A3}$$

Hence, (with $V'(z_{\min}) = 0$ and $V''(z_{\min}) = k(z_{\min})$) the shift due to the zero-point energy of the equilibrium distance at optimal separation is given by

$$z - z_{\min} = -\frac{\epsilon'(z_{\min})}{2k} = -\frac{\hbar k'(z_{\min})}{\sqrt{32mk^3}} \tag{A4}$$

For the 3-9 adsorption potential

$$k'(z_{\min}) = -\frac{2025}{\sqrt{10}}\frac{D}{\sigma^3} = -640.4\frac{D}{\sigma^3} \tag{A5}$$

Then, we find a relative shift in the equilibrium position

$$\frac{z - z_{\min}}{\sigma} = 0.51\frac{\hbar}{\sigma\sqrt{mD}} \tag{A6}$$

The dimensionless quantity $\hbar/(\sigma\sqrt{mD})$ is analogous to the De Boer quantum parameter in many-body physics, a measure of the relative importance of quantum effects. A typical value of the right side of eq A6 for ^{4}He, with $\sigma = 3$Å and $D = 10$K, is 0.36 so that $(z - z_{\min})/\sigma \approx 0.18$. While this might seem like a small relative change, it corresponds to an energy change (from eq A1) of $\Delta E = -k(z - z_{\min})^2 \approx -1.3D$. Such a large change means that the perturbation theory used to derive it is suspect. In fact, the preceding analysis exaggerates the magnitudes of ΔE because higher-order anharmonic terms reduce the shift, but that cannot be addressed analytically.

References and Notes

(1) Bruch, L. W.; Cole, M. W.; Zaremba, E. *Physical Adsorption: Forces and Phenomena*; Dover: Mineola, NY, 2007.

(2) *Microscopic Approaches to Quantum Liquids in Confined Geometries*; Krotscheck, E., Navarro, J., Eds.; World Scientific: Singapore, 2002.

(3) (a) Bonn, D.; Ross D. *Rep. Prog. Phys.* **2001**, *64*, 1085. (b) Barranco, M.; Guardiola, R.; Hernández, S.; Mayol, R.; Navarro, J.; Pi, M. *J. Low Temp. Phys.* **2006**, *142*, 1.

(4) Dash, J. G.; Schick, M.; Vilches, O. E. *Surf. Sci.* **1994**, *299/300*, 405.

(5) Bigelow, N.; Nacher, P. J.; Dupont-Roc, J. *J. Low Temp. Phys.* **1992**, *89*, 135.

(6) (a) Rossi, M.; Galli, D. E.; Reatto, L. *J. Low Temp. Phys.* **2007**, *146*, 95. (b) Boninsegni, M. *Phys. Rev. B* **2004**, *70*, 193411.

(7) (a) Cheng, E.; Cole, M. W.; Saam, W. F.; Treiner, J. *Phys. Rev. B* **1993**, *48*, 18214. (b) Cheng, E.; Cole, M. W.; Saam, W. F.; Treiner, J. *Rev. Mod. Phys.* **1993**, *65*, 557.

(8) (a) Gatica, S. M.; Stan, G.; Calbi, M. M.; Johnson, J. K.; Cole, M. W. *J. Low Temp. Phys.* **2000**, *120*, 337. (b) Stan, G.; Bojan, M. J.; Curtarolo, S.; Gatica, S. M.; Cole, M. W. *Phys. Rev. B* **2000**, *62*, 2173. (c) Shai, D. E.; Cole, M. W.; Lammert, P. E. *J. Low Temp. Phys.* **2007**, *147*, 59. (d) Urban, N. M.; Hernández, E. S.; Cole, M. W. *Phys. Rev. B* **2007**, in press; http://arxiv.org/abs/cond-mat/0702228.

(9) Goodstein, D. L. *States of Matter*; Dover: Mineola, NY, 1985; Chapter 5.

(10) McMillan, T.; Rutledge, J. E.; Taborek, P. *J. Low Temp. Phys.* **2005**, *138*, 995.

(11) Mistura, G.; Lee, H. C.; Chan, M. H. W. *J. Low Temp. Phys.* **1994**, *96*, 221.

(12) Nacher, P. J.; Dupont-Roc, J. *Phys. Rev. Lett.* **1991**, *67*, 2966.

(13) Ketola, K. S.; Wang, S.; Hallock, R. B. *Phys. Rev. Lett.* **1992**, *68*, 201.

(14) Hess, G. B.; Sabatini, M. J.; Chan, M. H. W. *Phys. Rev. Lett.* **1997**, *78*, 1739.

(15) Ancilotto, F.; Faccin, F.; Toigo, F. *Phys. Rev. B* **2000**, *62*, 17035.

(16) Chizmeshya, A.; Cole, M. W.; Zaremba, E. *J. Low Temp. Phys.* **1998**, *110*, 677.

(17) Hernando, A.; Hernandez, E. S.; Mayol, R.; Pi, M. *Phys. Rev. B* **2007**, submitted.

(18) Hernández, E. S.; Cole, M. W. *Phys. Rev. B* **2007**, *75*, 205421.

(19) Cole, M. W.; Tsong, T. T. *Surf. Sci.* **1977**, *69*, 325.

(20) Silvera, I. F. *Rev. Mod. Phys.* **1980**, *52*, 393.

(21) Boninsegni, M. *Phys. Rev. B* **2004**, *70*, 193411.

(22) Whitlock, P. A.; Chester, G. V.; Kalos, M. H. *Phys. Rev. B* **1988**, *38*, 2418.

(23) (a) Cazorla, C.; Boronat, J. *J. Low Temp. Phys.* **2004**, *134*, 43. (b) Giorgini, S.; Boronat, J.; Casulleras, J. *Phys. Rev. B* **1996**, *54*, 6099. (c) Okaue, Y.; Saiga, Y.; Hirashima, D. S. *J. Phys. Soc. Jpn.* **2006**, *75*, 053603.

(24) Results of G. Vidali presented in Figure 2.8 of ref 1 were derived from data of Mattera, L.; Rosatelli, F.; Salvo, C.; Tommasini, F.; Valbusa, U.; Vidali, G. *Surf. Sci.* **1980**, *93*, 515.

(25) (a) Derry, G.; Wesner, D.; Carlos, W.; Frankl, D. R. *Surf. Sci.* **1979**, *87*, 629. (b) Boato, G.; Cantini, P. *Adv. Electron. Electron Phys.* **1993**, *60*, 95; Hawkes, P. W., Ed. (c) Carlos, W. E.; Cole, M. W. *Surf. Sci.* **1980**, *91*, 339. (d) Elgin, R. L.; Goodstein, D. L. *Phys. Rev. A* **1974**, *9*, 2657.

(26) (a) Annett, J. F.; Cole, M. W.; Shaw, P. B.; Stratt, R. M. *J. Low Temp. Phys.* **1991**, *84*, 1. (b) For a more detailed variational study, see: Carraro, C.; Cole, M. W. *Phys. Rev. B* **1992**, *46*, 10947. The interactions used in that study have been superceded.

(27) (a) Klier, J.; Wyatt, A. F. G. *J. Low Temp. Phys.* **1998**, *113*, 817. (b) Klier, J.; Wyatt, A. F. G. *Phys. Rev. B* **2002**, *65*, 212504.

(28) Phillips, J. A.; Ross, D.; Taborek, P.; Rutledge, J. E. *Phys. Rev. B* **1998**, *58*, 3361.

(29) (a) Demolder, B.; Bigelow, N.; Nacher, P. J.; Dupont-Roc, J. *J. Low Temp. Phys.* **1995**, *98*, 91. (b) Demolder, B.; Dupont-Roc, J. *J. Low Temp. Phys.* **1996**, *104*, 359. (c) Ross, D.; Phillips, J. A.; Rutledge, J. E.; Taborek, P. *J. Low Temp. Phys.* **1997**, *106*, 829.

(30) Pricaupenko, L.; Treiner, J. *Phys. Rev. Lett.* **1994**, *72*, 2215. Their D values are semiempirical, approximately 20% higher than the ab initio values of ref 16.

(31) (a) Miller, M. D.; Nosanow, L. H. *J. Low Temp. Phys.* **1978**, *32*, 145. (b) Brami, B.; Joly, F.; Lhuillier, C. *J. Low Temp. Phys.* **1994**, *94*, 63.

(32) Boninsegni, M.; Cole, M. W.; Toigo, F. *Phys. Rev. Lett.* **1999**, *83*, 2002.

(33) Ross, D.; Taborek, P.; Rutledge, J. E. *Phys. Rev. B* **1998**, *58*, R4274.

(34) Cheng, E.; Mistura, G.; Lee, H. C.; Chan, M. H. W.; Cole, M. W.; Carraro, C.; Saam, W. F.; Toigo, F. *Phys. Rev. Lett.* **1993**, *70*, 1854.

(35) Shi, W.; Johnson, J. K.; Cole, M. W. *Phys. Rev. B* **2003**, *68*, 125401.

(36) Curtarolo, S.; Stan, G.; Bojan, M. J.; Cole, M. W.; Steele, W. A. *Phys. Rev. B* **2000**, *61*, 1670.

(37) Rutledge, J. E.; Taborek, P. *J. Low Temp. Phys.* **1994**, *95*, 405.

(38) Schmeits, M.; Lucas, A. A. *Surf. Sci.* **1977**, *64*, 176.

(39) (a) Boninsegni, M.; Moroni, S. *J. Low Temp. Phys.* **2000**, *118*, 1. (b) Krotscheck, E.; Miller, M. D.; Wojdylo, J. *Phys. Rev. B* **1999**, *60*, 13028. (c) Krotscheck, E.; Miller, M. D. *Phys. Rev. B* **1999**, *60*, 13038.
(40) Gordillo, M. C.; Boronat, J.; Casulleras, J. *Phys. Rev. Lett.* **2000**, *85*, 2348.
(41) Stan, G.; Cole, M. W. *Surf. Sci.* **1998**, *395*, 280.
(42) Schmeits, M.; Lucas, A. A. *Prog. Surf. Sci.* **1983**, *14*, 1.
(43) Cole, M. W.; Schmeits, M. *Surf. Sci.* **1978**, *75*, 529.
(44) Lucas, A. A.; Ronveaux, A.; Schmeits, M.; Delanaye, F. *Phys. Rev. B* **1975**, *12*, 5372.
(45) Johnson, S. A.; Olliver, P. J.; Mallouk, T. E. *Science* **1999**, *283*, 963.